

**This is the preprint version of the contribution published as:**

**Escher, B.I., Glauch, L., König, M., Mayer, P., Schlichting, R.** (2019):  
Baseline toxicity and volatility cutoff in reporter gene assays used for high-throughput  
screening  
*Chem. Res. Toxicol.* **32** (8), 1646 – 1655

**The publisher's version is available at:**

<http://dx.doi.org/10.1021/acs.chemrestox.9b00182>

# **Baseline toxicity and volatility cut-off in reporter gene assays used for high-throughput screening**

Beate I. Escher,<sup>†‡\*</sup> Lisa Glauch,<sup>†</sup> Maria König,<sup>†</sup> Philipp Mayer<sup>§</sup> and Rita Schlichting<sup>†</sup>

<sup>†</sup>Department of Cell Toxicology, Helmholtz Centre for Environmental Research – UFZ, Permoserstr. 15, DE-04318 Leipzig, Germany,

<sup>‡</sup>Environmental Toxicology, Center for Applied Geoscience, Eberhard Karls University Tübingen, Hölderlinstr. 12, DE-72074 Tübingen, Germany

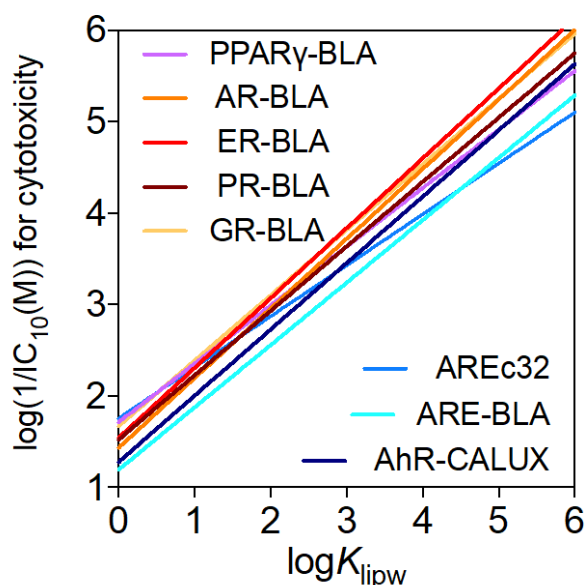
<sup>§</sup>Department of Environmental Engineering, Technical University of Denmark, Bygningstorvet 115, DK-2800 Kongens Lyngby, Denmark

\*Address correspondence to: [beate.escher@ufz.de](mailto:beate.escher@ufz.de)

## Key words

Cell-based bioassays, reporter gene assays, high-throughput screening, narcosis, quantitative structure activity relationship, QSAR, volatility cut-off

## Table of Contents (TOC) graphic



## ABSTRACT

Most studies using high-throughput *in vitro* cell-based bioassays tested chemicals up to a certain fixed concentration. It would be more appropriate to test up to concentrations predicted to elicit baseline toxicity because this is the minimal toxicity of every chemical. Baseline toxicity is also called narcosis and refers to nonspecific intercalation of chemicals in biological membrane leading to loss of structure of membranes and impaired functioning of membrane-related processes such as mitochondrial respiration. In cells baseline toxicity manifests as cytotoxicity, which was quantified by a robust live-cell imaging method. Inhibitory concentrations for baseline toxicity varied by orders of magnitude between chemicals and were described by a simple quantitative structure activity relationship (QSAR) with the liposome-water partition constant as sole descriptor. The QSAR equations were remarkably similar for eight reporter gene cell lines of different cellular origin, six of which were used in Tox21. Mass-balance models indicated constant critical membrane concentrations for all cells and all chemicals with a mean of  $69 \text{ mmol}\cdot\text{kg}_{\text{lip}}^{-1}$  (95%CI: 49 to 89), which is in the same

range as for bacteria and aquatic organisms and consistent with the theory of critical membrane burden of narcosis. The challenge of developing baseline QSARs for cell lines is that many confirmed baseline toxicants are rather volatile. We deduced from cytotoxicity experiments with (semi)volatile chemicals that only chemicals with medium-air partition constants  $>10000$  L/L can be tested in standard robotic setups without appreciable loss of effect. Chemicals just below that cut-off showed cross-over effects in neighboring wells, whereas the effects of chemicals with lower medium-air partition constants were plainly lost. Applying the “volatility cut-off” to  $>8000$  chemicals tested in Tox21 indicated that approximately 20% of Tox21 chemicals could have partially been lost during the experiments. We recommend applying the baseline QSARs together with volatility cut-offs for experimental planning of reporter gene assays, i.e., to dose only chemicals with medium-air partition constants  $> 10000$  at concentrations up to the baseline toxicity level.

## INTRODUCTION

The advent of high-throughput screening (HTS) with reporter gene assays has been instrumental for the shift towards *in vitro* methods in toxicity testing and risk assessment.<sup>1, 2</sup> For quantitative *in vitro* to *in vivo* extrapolation,<sup>3</sup> a comprehensive exposure assessment with measured freely dissolved concentrations in cell-based bioassays would be ideal. In 24-, 48- and 96-well plates, solid-phase microextraction methods have been implemented to quantify the freely dissolved concentrations of selected chemicals in cell-based bioassays,<sup>4, 5</sup> but it is not feasible yet to measure concentrations in 384- and 1536-well plates on a routine basis for the ten thousands of chemicals screened in programs like Tox21.<sup>6</sup> For effect assessment of environmental samples, such as surface water, wastewater, sediment, biota and human biomonitoring, we are faced with thousands or more diverse chemicals in one sample and there is no way to quantify them all analytically in all types of environmental samples, let alone in the bioassays. Provided we can transfer environmental mixtures in a defined way into the cellular test system,<sup>7</sup> we can estimate freely dissolved and cellular concentrations over the exposure time of an experiment by application of established mass balance models<sup>8, 9</sup> and kinetic information of cellular uptake<sup>10</sup> and binding to the multi-well plate.<sup>11</sup>

There remain two major issues that impede the implementation of HTS reporter gene assays in risk assessment and these refer to the loss of chemicals to the air in

common HTS setups and the need to define minimal toxicity (baseline toxicity). The latter is needed to define appropriate dosing concentrations and to interpret the cytotoxicity burst, which refers to the observation that, at concentrations close to cytotoxicity, cells activate numerous defense mechanisms, potentially leading to non-specific activation of reporter genes.<sup>12, 13</sup> Many different methods for cytotoxicity assessment<sup>14</sup> exist but not all of them are suitable for routine HTS.<sup>15</sup> Cytotoxicity assays are typically based on staining of cells or by quantifying metabolic function but artifacts are abundant,<sup>15</sup> especially when it comes to testing mixtures of environmental samples. We apply here a much simpler method, based on live-cell imaging, which is non-invasive and well compatible with testing of environmental samples.<sup>16</sup>

There are diverse set ups to dose volatile chemicals via the air phase in cell-based bioassays,<sup>17</sup> some of which were designed specifically for dosing via the air-liquid interface and most commonly applied to expose lung cells to aerosols and fine particles.<sup>18</sup> Mass balance models have also been applied to estimate the exposure in air-liquid interface cell system.<sup>19, 20</sup> None of these exposure systems are amenable to HTS using multi-well plates that are just covered with a plastic lid or a breathable sealant plus a plastic lid.

Semi-volatile organic chemicals are hard to dose via classical air-exposure systems because they are not volatile enough but they may still get lost or cause cross-contaminations in HTS bioassays. This grey zone remains to be clearly defined. Classic cellular bioassays dosed via the aqueous phase can also be set up without head-space, which is fairly easy for bacterial assays<sup>21</sup> but more challenging for the HTS bioassays in multi-well plates, where airtight systems are tedious and only work manually with syringe injections of the chemical to be dosed and minimal headspace, thereby typically compromising the cell viability and performance of the assay.<sup>22</sup> We have previously proposed an empirical “volatility cut-off” around a Henry constant of  $10^{-6} \text{ atm m}^3 \text{ mol}^{-1}$ , corresponding to an air-water partition constant  $K_{a/w}$  of  $4 \cdot 10^{-5} \text{ L/L}$  at  $37^\circ\text{C}$  (310K).<sup>23</sup> This cut-off was derived from a mass balance model expanded from Liu et al.<sup>20</sup> also accounting for binding of chemicals to medium proteins and lipids. A better determinant for the loss of effects of (semi)volatile chemicals is expected to be the medium-air partition constant ( $K_{\text{medium/air}}$ ), and the terms “volatility cut-off” and “Henry constant cut-off” seem thus not optimal. An empirical  $K_{\text{medium/air}}$  cut-off for effect losses due to evaporative losses of semi-volatile chemicals in standard test systems will thus be developed in this study. This will be accomplished by observing loss of

effects and cross-over of effects to other wells in combination with mass balance modelling.

In this study we opted against quantification of the exposure concentration in the cell assays. To measure loss processes in HTS systems by chemical analysis, we would have to modify the setup, which would not be a realistic HTS scenario. Hence we decided to quantify loss processes as loss of effect. While solid-phase microextraction (SPME) methods have been developed<sup>24</sup> for this purpose and a practical workflow has been demonstrated using 96-well plates and reporter gene bioassays,<sup>5</sup> any measurement would interfere with the practical bioassay workflow of a typical cell-based bioassay. In an accompanying study Birch et al.<sup>25</sup> have measured the losses and cross-over of 24 volatile and semi-volatile chemicals from 3 different cell culture media in 96-well plates without cells. Both approaches taken together provided a strong line of evidence what is practically feasible. While exploring the domain of applicability, we also compared different dosing strategies, comparing conventional dosing using pipettes with dosing using a digital dispenser.<sup>26</sup>

Quantitative structure-activity relationships (QSAR) for prediction of baseline toxicity based on biomembrane-water partitioning constants (or proxies thereof, such as the octanol-water or liposome-water partition constant) have been developed for many aquatic organisms. Vaes et al.<sup>27</sup> developed a QSAR for non-polar and polar narcotics towards guppy fish with measured liposome-water partition constants  $K_{ip/w}$ <sup>28</sup> for 19 confirmed baseline toxicants (8 non-polar and 11 polar chemicals). They demonstrated that there is no difference in baseline toxicity between non-polar and polar chemicals and henceforth many groups have developed general baseline toxicity QSARs based on  $K_{ip/w}$ <sup>29, 30</sup> and the concept was also expanded to ionizable compounds by applying the ionization-corrected  $D_{ip/w}(pH)$ .<sup>31-33</sup>

This group of 19 confirmed baseline toxicants was used to develop baseline toxicity QSARs for diverse reporter gene cell lines after those chemicals were excluded that would not pass the  $K_{medium/air}$  cut-off. Another goal was to derive the critical membrane concentration for baseline toxicity in reporter gene cell lines. Each experimental nominal concentration can be converted to critical membrane concentration by mass balance modelling to check if baseline toxicity is uniform across cells. Provided we can confirm constant critical membrane concentrations, the mean of the critical membrane concentrations can be used to predict nominal cytotoxic concentrations and construct baseline toxicity QSAR for any given cell line and assay medium. Although baseline

toxicity constitutes the minimal toxicity any chemical has, it is important to know it, in order to define how specific effects are and to improve the planning of the dosing in HTS.

## MATERIALS AND METHODS

**Chemicals.** The 19 chemicals from the original set of the Vaes et al.<sup>27</sup> were considered in this study (Table 1). This set of chemicals had been used to set up a baseline toxicity (narcosis) QSAR based on measured  $K_{lipw}$ <sup>28</sup> as chemical descriptor.

All chemicals in Table 1 were evaluated in the mass balance model, those with  $K_{a/w} < 0.1$  L/L were tested experimentally (Table S1), and those that passed the  $K_{medium/air}$  cut-off of  $10^4$ , which was derived experimentally as further detailed below, were included in the QSAR development.

**Physicochemical Properties.** The liposome-water partition constants  $K_{lip/w}$  were experimentally determined by Vaes et al.<sup>28</sup> at 288 K using L- $\alpha$ -dimyristoylphosphatidylcholine as a model for membrane lipids (Table 1). Given the small temperature difference of only 2 K to the temperature, at which cell assays were performed (290 K), and because of the generally low temperature dependence of partition constants between condensed phases,<sup>34</sup> we did not apply a temperature correction. Bovine serum albumin served as surrogate for cell and medium proteins and the partition constants between proteins and water  $\log K_{protein/w}$  were estimated by a linear-solvation energy relationship (LSER) using equation 1 from Endo et al.<sup>35</sup> and the chemical descriptors from the UFZ LSER database<sup>36</sup> (Table 1).

The air-water partition constants  $K_{a/w}$  at 290K (Table 1) were determined from van't Hoff plots of  $\log K_{a/w}$  against  $1/T$ , where the temperature dependence of Henry's law constant was estimated with the LSER given by Goss et al.<sup>37</sup>

The partitioning between assay medium and water  $K_{medium/w}$  (Table 1) was calculated by a mass balance model for three types of media that were used for the bioassays. AhR-CALUX and AREc32 cells were tested in 90% DMEM and 10% FBS (volume fraction  $V_{f_w} = 99.09$  %,  $V_{f_{lip}} = 0.0139$  %,  $V_{f_{protein}} = 0.89$  %) <sup>5</sup>, ARE-BLA was tested in 90% DMEM and 10% dialyzed FBS (dFBS; assuming the same  $V_{f_{lip}}$  and  $V_{f_{protein}}$  as for AhR-CALUX and AREc32) and the assay medium for all other GeneBLazer cell lines was 98% Opti-MEM supplemented with 2% charcoal-stripped FBS (csFBS;  $V_{f_w} = 99.51$  %,  $V_{f_{lip}} = 0.0023$  %,  $V_{f_{protein}} = 0.49$  %) <sup>5</sup>.

The  $K_{\text{medium/w}}$  were calculated with eq. 1 from the volume fractions  $V_f$  of lipids ( $V_{f_{\text{lip}}}$ ), proteins ( $V_{f_{\text{protein}}}$ ) and water ( $V_{f_w}$ ) and the partition constants between lipids and water ( $K_{\text{lip/w}}$ ) and proteins and water ( $K_{\text{protein/w}}$ ).

$$K_{\text{medium/w}} = V_{f_{\text{lip,medium}}} K_{\text{lip/w}} + V_{f_{\text{protein,medium}}} K_{\text{protein/w}} + V_{f_{w,medium}} \quad (1)$$

The partition constants between medium and air  $K_{\text{medium/air}}$  were calculated with Hess' law (eq. 2).

$$K_{\text{medium/air}} = \frac{K_{\text{medium/w}}}{K_{a/w}} \quad (2)$$



1 Table 1. Chemicals tested and their partition constants between liposomes and water  $K_{lip/w}$ , protein and water  $K_{protein/w}$ , air and water  $K_{a/w}$  as well as between medium and water  
 2  $K_{medium/w}$  and medium and air  $K_{medium/air}$ . The column “HTS setup?” indicates if the chemical can be safely run under HTS conditions (marked with yes), or not (marked with no). In  
 3 the column “Included in QSAR?” the chemicals that were the training set of the QSAR are indicated and the “additional” refers to chemicals that were used to validate the applicability  
 4 domain for the QSAR. In the column “polarity” we indicate the previous classification for polar and non-polar chemicals from the initial set of Vaes’ baseline toxicants.<sup>27</sup> The chemicals  
 5 are sorted from high to low  $K_{medium/air}$  (calculated by eq. 1 and 2 without further temperature correction). Further information on the tested chemicals is given in the SI, Table S1.

Chemical	HTS setup?	Included in QSAR?	Polarity	$\log K_{lip/w}$ [L/L] <sup>28</sup>	$\log K_{protein/w}$ [L/L] LSER	$\log K_{a/w}$ [L/L] LSER	$\log K_{medium/w}$ [L/L] <sup>a</sup>	$\log K_{medium/w}$ [L/L] <sup>b</sup>	$\log K_{medium/air}$ [L/L] <sup>a</sup>	$\log K_{medium/air}$ [L/L] <sup>b</sup>
Temperature				288 K	290 K	290 K				
2-Phenylphenol	yes	training set	polar	3.46	2.99	-5.87	1.01	0.76	6.88	6.64
3-Nitroaniline	yes	training set	polar	2.17	2.13	-6.00	0.35	0.22	6.35	6.22
4-Chloro-3-methylphenol	yes	training set	polar	3.34	2.80	-4.52	0.84	0.61	5.36	5.14
4-Pentylphenol	yes	training set	polar	4.31	3.55	-3.77	1.55	1.27	5.31	5.03
2-Allylphenol	yes	training set	polar	3.06	2.46	-4.05	0.57	0.38	4.62	4.43
2,4,5-Trichloroaniline	yes	training set	polar	4.16	3.40	-3.05	1.41	1.13	4.46	4.19
2-Butoxyethanol	yes	training set	non-polar	0.60	0.71	-4.24	0.02	0.01	4.25	4.24
Aniline	no	excluded	polar	1.63	1.39	-3.82	0.08	0.05	3.91	3.87
Quinoline	no	excluded	polar	1.67	1.77	-3.68	0.18	0.11	3.86	3.79
Butan-1-ol	no	additional	non-polar	0.45	0.91	-3.03	0.03	0.01	3.06	3.05
Pentan-3-ol	no	additional	non-polar	0.995	1.00	-2.89	0.03	0.02	2.92	2.91
Nitrobenzene	no	additional	polar	2.01	1.99	-2.71	0.28	0.17	2.99	2.88
Hexan-1-ol	no	additional	non-polar	1.91	1.71	-2.75	0.16	0.10	2.92	2.85
2-Nitrotoluene	no	additional	polar	2.41	2.34	-2.48	0.48	0.32	2.96	2.80
N,N-Dimethylaniline	no	additional	polar	2.33	2.09	-2.33	0.33	0.20	2.66	2.53
2,4,5-Trichlorotoluene	no	excluded	non-polar	4.77	3.96	-0.61	1.96	1.67	2.57	2.28
1,3,5-Trichlorobenzene	no	excluded	non-polar	3.95	3.55	-0.36	1.53	1.27	1.89	1.62
Chlorobenzene	no	excluded	non-polar	2.81	2.53	-0.51	0.61	0.42	1.12	0.93
p-Xylene	no	Excluded	non-polar	2.98	2.64	-0.32	0.70	0.50	1.03	0.82

6 <sup>a</sup>90% DMEM with Glutamax and 10% FBS; <sup>b</sup>98% OptiMEM and 2% cs-FBS.

7

8 **Cell Lines.** The reporter gene assays and the cell line they were derived from are  
 9 listed in Table 2. The GeneBLAzer cell lines<sup>38,39</sup> were obtained from Thermo Fisher  
 10 (Schwerte, Germany), AREc32 cells<sup>40</sup> by courtesy of C. Roland Wolf, Cancer research  
 11 UK, and AhR-CALUX cells<sup>41</sup> by courtesy of Michael Denison, UC Davis, USA. 30  $\mu$ L  
 12 of cell suspension containing the number of cells given in Table 2 were plated in each  
 13 well of a black 384-well polystyrene microtiter plate with clear bottom (AREc32 #3764,  
 14 all other cell lines BioCoat # 356663, Corning, Maine, USA) using a Multiflow  
 15 Dispenser (Biotek, Vermont, USA) followed by 24h incubation at 37°C and 5% CO<sub>2</sub>.

16 Previous experiments have demonstrated that these cells need 24h to adhere  
 17 and to adapt to the new environment. Thus, the cell number stays virtually constant  
 18 during that time<sup>10</sup> and we used the number of cells plated as the starting cell number.  
 19 We measured the confluency of the cell layer in the plate directly before dosing  
 20 corresponding to 24 h after seeding and again after 24 $\pm$ 2 h after dosing. The average  
 21 of the confluency was used to estimate the final cell number. The average of the  
 22 difference between the plated cell number and the estimated final cell number was  
 23 used for modeling (mean cell number in assay). The total volume of the cells in Table  
 24 2 and the volume fraction of water  $V_{f,w,cell}$ , proteins  $V_{f,protein,cell}$  and lipid  $V_{f,lipid,cell}$  of the  
 25 GeneBLAzer cell lines were taken from Fischer et al.<sup>9</sup> and of AREc32 and AhR-CALUX  
 26 from Henneberger et al.<sup>24</sup> The partition constants between cells and water (eq. 3) were  
 27 calculated in analogy to the medium-water partitioning (eq. 1).

$$28 \quad K_{cell/w} = V_{f,lip,cell} K_{lip/w} + V_{f,protein,cell} K_{protein/w} + V_{f,w,cell} \quad (3)$$

29

30 *Table 2. Reporter gene cell lines evaluated and numbers of cells plated and averaged during the experiment in*  
 31 *384-well plates as well as the total volume of the cells and the apportionment into water, lipid and protein phases.*

Reporter gene cell line	Derived from	Number of plated cells/well	Estimated mean cell number in assay <sup>a</sup>	Total volume of cells $V_{cell}$ (nL)	$V_{f,water,c}$ <sub>ell</sub>	$V_{f,protein,c}$ <sub>ell</sub>	$V_{f,lipid,c}$ <sub>ell</sub>
AREc32	MCF7	2500	4300 $\pm$ 290	16.8	94.4% <sup>c</sup>	5.1% <sup>c</sup>	0.5% <sup>c</sup>
ARE-BLA	HepG2	5500	5820 $\pm$ 310	18.2	87.4% <sup>b</sup>	9.5% <sup>b</sup>	3.2% <sup>b</sup>
AhR-CALUX (H4L7.5c2)	H4Ile	3000-3250	5360 $\pm$ 750	21.8	93.9% <sup>c</sup>	5.5% <sup>c</sup>	0.6% <sup>c</sup>
PPAR $\gamma$ -BLA	HEK293H	4500-5500	5940 $\pm$ 760	15.7	88.7% <sup>b</sup>	8.0% <sup>b</sup>	3.4% <sup>b</sup>
AR-BLA	HEK293T	4500-5000	5650 $\pm$ 580	331.8	90.6% <sup>b</sup>	8.4%	1.0% <sup>b</sup>

ER $\alpha$ -BLA	HEK293T	3500-4250	5110 $\pm$ 460	35.3	90.6% <sup>b</sup>	8.4% <sup>b</sup>	1.0% <sup>b</sup>
PR-BLA	HEK293T	4500-4750	5870 $\pm$ 450	41.4	90.6% <sup>b</sup>	8.4% <sup>b</sup>	1.0% <sup>b</sup>
GR-BLA	HEK293T	4500-5000	6410 $\pm$ 450	45.0	90.6% <sup>b</sup>	8.4% <sup>b</sup>	1.0% <sup>b</sup>

32 <sup>a</sup>average between plated cells and final cell number after 24 h of exposure; <sup>b</sup>Fischer et al.;<sup>9</sup>

33 <sup>c</sup>Henneberger et al.<sup>24</sup>

34

35 **Assay Medium.** All cell lines were grown as described in previous work.<sup>42-44</sup> For the  
36 cytotoxicity assay we switched from growth medium to assay medium that was  
37 composed of 90% DMEM Glutamax with 10% FBS for AREc32 and AhR-CALUX, 90%  
38 DMEM with 10% dFBS and 0.1 mM NEAA und 25 mM HEPES for ARE-BLA and 98%  
39 Opti-MEM with 2% cs-FBS for all other GeneBLAzer cell lines. 100 U/mL Penicillin and  
40 100  $\mu$ g/mL Streptomycin were supplemented to the media. All media and FBS were  
41 purchased from Thermo Fisher (Schwerte, Germany).

42

43 **Dosing Procedures.** Liquid chemicals were dosed into medium as neat compounds.  
44 Of the baseline toxicants, only 3-Nitroaniline, 2,4,5-Trichloroaniline and 2-  
45 Phenylphenol were solids as well as the seven additional test chemicals and 20 mM  
46 to 0.5 M stock solutions were prepared in DMSO.

47 The dosing plates were prepared by dispensing different volumes of the liquids  
48 or DMSO stock solutions into 120  $\mu$ L medium in 96-well plates using a Tecan D300e  
49 Digital Dispenser (Tecan, Crailsheim, Germany). Technical details and diverse  
50 bioassay applications of this dispenser that is based on inkjet technology are provided  
51 in the literature.<sup>26, 45, 46</sup> The dosing plates were sealed and shaken for 5-10 seconds  
52 prior to the dosing step.

53 The diluted test chemicals were dosed in duplicates by transferring two times  
54 10  $\mu$ L from two 96-well dosing plates into a 384-well plate that contained 30  $\mu$ L medium  
55 and the number of cells given Table 2, using a 96-pipette head (Hamilton Microlab  
56 Star, Bonaduz, Switzerland). In routine HTS set up of the assays, a lid is placed on  
57 the plates during incubation. If no further information was given, this was the  
58 experimental set up of this study. We also evaluated if the loss of chemicals was  
59 reduced if the plate was sealed by a breathable foil (Biozym, Hessisch Oldendorf,  
60 Germany) during incubation for 24h.

61 For comparison, the dosing plates were also prepared with a Hamilton Robot  
62 (Star, Hamilton, Bonaduz, Switzerland) as previously described.<sup>44</sup> Briefly, for each  
63 chemical, 45 $\mu$ L of the chemical dissolved in assay medium were transferred from the

64 dosing vials into 45  $\mu\text{L}$  of assay medium in one well of a clear 384-well plate (Corning,  
65 Maine, USA) followed by a 11-step serial dilution with a 1:2 dilution between each step.  
66 10 $\mu\text{L}$  of the diluted samples were dosed into 384-well plate containing 30 $\mu\text{L}$  of medium  
67 with the cell numbers given in Table 2. A detailed visualization of the bioassay workflow  
68 is given in the SI, Section S2, Figure S1.

69  
70 **Quantification of Cytotoxicity.** The confluency as a surrogate for the number of cells  
71 in each well of the 384-well plates was measured immediately before dosing and again  
72 after another 24h incubation at 37°C and 5% CO<sub>2</sub> using an IncuCyte S3 live cell  
73 imaging system (Essen BioScience, Ann Arbor, Michigan, USA). Image analysis of the  
74 confluency of the cell layer was performed using the IncuCyte S3 software, that  
75 provides tools for image processing and quantitative analysis. A method for analysis  
76 for each cell line was defined using a training set of images with different confluency  
77 (see Section S3 in the SI and Figure S2 for more details). Confluency served as  
78 surrogate for cell viability and proliferation and was expressed as “% inhibition of cell  
79 viability” as compared to unexposed cells.

$$80 \quad \% \text{ Inhibition of cell viability} = 100\% - \frac{\% \text{ confluency (exposed cells)}}{\% \text{ confluency (unexposed cells)}} \quad (4)$$

81 The SI, Section S4 and Figure S3, provides a comparison of cell viability testing using  
82 the Presto Blue<sup>®</sup> assay and the cell imaging. The live-cell imaging method has been  
83 used for cytotoxicity assessment of water samples in previous studies.<sup>16, 47</sup> We further  
84 compared the dosing by the digital dispenser of DMSO stocks and dosing of methanol  
85 stocks with automated pipetting (SI, Section S5, Figures S4 and S5) and found no  
86 differences, hence all concentration-response curves of a given chemical were  
87 evaluated together.

88 The inhibitory concentration for 10% reduction of cell viability/growth, i.e.  
89 cytotoxicity, IC<sub>10</sub>, was determined from the linear portion of the concentration-response  
90 curve, which is below 30-40% inhibition.<sup>48</sup> The IC<sub>10</sub> was calculated from the slope of  
91 the regression of % inhibition of cell viability against the dosed (nominal) concentration  
92 with eq. 5 and the standard error of IC<sub>10</sub> was calculated with eq. 6.

$$93 \quad \text{IC}_{10} = \frac{10\%}{\text{slope}} \quad (5)$$

$$94 \quad \text{SE}(\text{IC}_{10}) \approx \frac{10\%}{\text{slope}^2} \cdot \text{SE}(\text{slope}) \quad (6)$$

95 The IC<sub>10</sub> of DMSO are given for reference in the SI, Table S2.

96 **Baseline toxicity QSAR.** Baseline toxicity QSAR of the form given in eq. 7 were set  
 97 up for all cell lines from a regression of experimental  $\log(1/IC_{10})$  against  $\log K_{ip/w}$ .

$$98 \log(1/IC_{10}(M)) = \text{slope} \cdot \log K_{ip/w} + \text{intercept} \quad (7)$$

99

100 **Mass balance model for 384-well plates with head space.** We expanded the mass  
 101 balance model developed previously<sup>9</sup> by an additional air compartment analogously to  
 102 Liu et al.<sup>20</sup> Additional loss processes in HTS bioassays include binding to the plastic of  
 103 the well plates and degradation. Binding to the plastic of the well plates was determined  
 104 to be negligible under the test conditions.<sup>11</sup> The baseline toxicants used here were  
 105 stable in other toxicity experiments<sup>27</sup> over longer duration, so we did not check stability  
 106 in the present study.

107 The resulting mass balance equations for the fraction in air,  $f_a$ , in medium,  $f_{\text{medium}}$  and  
 108 in the cells,  $f_{\text{cell}}$ , is given by eqs. (8-10).

$$109 f_a = \frac{1}{1 + \frac{K_{\text{cell/w}} V_{\text{cell}}}{K_{a/w} V_a} + \frac{K_{\text{medium/w}} V_{\text{medium}}}{K_{a/w} V_a}} \quad (8)$$

110

$$111 f_{\text{medium}} = \frac{1}{1 + \frac{K_{\text{cell/w}} V_{\text{cell}}}{K_{\text{medium/w}} V_{\text{medium}}} + \frac{K_{a/w} V_a}{K_{\text{medium/w}} V_{\text{medium}}}} \quad (9)$$

112

$$113 f_{\text{cell}} = \frac{1}{1 + \frac{K_{\text{medium/w}} V_{\text{medium}}}{K_{\text{cell/w}} V_{\text{cell}}} + \frac{K_{a/w} V_a}{K_{\text{cell/w}} V_{\text{cell}}}} \quad (10)$$

114

115 The cellular inhibitory concentration  $IC_{10,\text{cell}}$  can then be predicted from the nominal  
 116 inhibitory concentration  $IC_{10}$  by multiplying with  $f_{\text{cell}}$  and correcting for the volume ratios  
 117 (eq. 11).

$$118 IC_{10,\text{cell}} = IC_{10} \cdot f_{\text{cell}} \cdot \frac{V_{\text{medium}} + V_{\text{cell}}}{V_{\text{cell}}} \quad (11)$$

119

120 **Critical Membrane Concentrations.** Within the cell compartment, the fraction in the  
 121 membrane of the cell  $f_{lip,\text{cell}}$  can be calculated with eq. 12. For simplicity, we use the  
 122 liposome water partition constant  $K_{ip/w}$  as the partition constant representative for all  
 123 cellular lipids.

$$124 f_{lip,\text{cell}} = \frac{1}{1 + \frac{1}{K_{ip/w} V_{lip,\text{cell}}} + \frac{K_{\text{protein/w}} V_{\text{protein,cell}}}{K_{ipw} V_{lip,\text{cell}}}} \quad (12)$$

125 The critical membrane concentration  $IC_{10,membrane}$  can then be derived from  $f_{lip,cell}$  and  
126  $IC_{10,cell}$  by accounting also for the volumes of lipids in cells  $V_{lipid,cell}$  (Table 2).

$$127 \quad IC_{10,membrane} = IC_{10,cell} \cdot \frac{f_{lip,cell}}{V_{lipid,cell}} \quad (13)$$

128  
129 **Prediction of  $K_{medium/air}$  for Tox21 chemicals.** The names and physicochemical  
130 properties of 8947 chemicals tested in Tox21<sup>49</sup> were retrieved from the Chemistry  
131 Dashboard of the UP EPA<sup>50</sup> The  $K_{a/w}$  was calculated from the  $K_{ow}$  and  $K_{oa}$  that had  
132 been predicted with OPERA.<sup>51</sup> We calculated the  $K_{medium/air}$  from  $K_{medium/w}$  and  $K_{a/w}$   
133 assuming a medium that contains 10% FBS. For screening purposes, the  $K_{medium/w}$  can  
134 be estimated by very simple QSARs and a mass balance model (eq. 14) that only  
135 require the  $K_{ow}$  as sole input parameter to estimate protein binding  $K_{protein/w}$  and lipid  
136 partitioning  $K_{lip/w}$ , together with some information on the medium composition.<sup>52</sup>

$$137 \quad K_{medium/w} = 0.0046 \cdot K_{protein/w} + 0.00015 \cdot K_{lip/w} + 0.99525$$
$$138 \quad = 0.0046 \cdot 10^{0.71 \cdot \log K_{ow} + 0.42} + 0.00015 \cdot 10^{1.01 \cdot \log K_{ow} + 0.12} + 0.99525 \quad (14)$$

139 This equation holds only for neutral organic chemicals but was nevertheless applied to  
140 all chemicals in Tox21 irrespective of their speciation.

## 141 RESULTS AND DISCUSSION

142 **Loss processes to the air and cross-contamination of neighboring wells.** For the  
143 standard HTS set up, we previously proposed a “volatility cut-off” corresponding to a  
144 Henry constant of  $10^{-6} \text{ atm} \cdot \text{m}^3 \cdot \text{mol}^{-1}$ , corresponding to a  $K_{a/w}$  of approximately  $4 \cdot 10^{-5}$   
145 ( $\log K_{a/w} -4.4$ ).<sup>23</sup> Here we explored this cut-off in more detail and if chemicals can cross-  
146 contaminate neighboring wells. To this end we dosed only the middle six rows of a  
147 384-well plates with a dilution series of one chemical per plate and added medium only  
148 to the remaining rows. Detailed results are described in Section S6 of the SI. Briefly,  
149 Butoxyethanol ( $\log K_{a/w} -4.24$ ) showed uniform cytotoxicity in all wells dosed with the  
150 same concentration and no effects in neighboring unexposed wells (Figure S6A).  
151 Pentan-3-ol ( $\log K_{a/w} -2.89$ ) clearly showed a loss of cytotoxicity (Figure S6B) and N,N-  
152 Dimethylaniline ( $\log K_{a/w} -2.33$ ) cross-contaminated the unexposed wells or wells  
153 dosed with lower levels (Figure S6C).

154 Sealing the plate with a breathable foil instead of just placing a lid did not change  
155 the picture for Butoxyethanol but reduced the loss of effect for the two more volatile  
156 chemicals, however, could not avoid the cross-contamination of neighboring wells

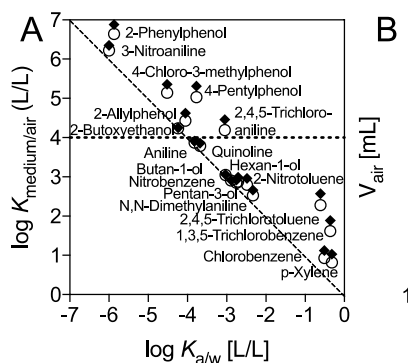
157 (Figure S6). In the accompanying paper,<sup>25</sup> sealing did not reduce loss of chemicals but  
158 reduced cross-over.

159 The test chemicals were ranked in Table 1 according to their  $K_{\text{medium/air}}$ .  
160 Butoxyethanol had the lowest  $\log K_{\text{medium/air}}$  of 4.24/4.25 of all chemicals that appeared  
161 still retained in the plate during the experiment and therefore we tentatively defined a  
162  $K_{\text{medium/air}}$  cut-off of  $10^4$ , which is evaluated more systematically in the next section.

163

164 **Loss processes to the air: defining the physicochemical applicability domain of**  
165 **HTS reporter gene assays.** The loss processes to air were not only determined by  
166 the volatility or vapor pressure of the compounds or the Henry constant but also by  
167 how much the medium components and cells retain the chemical and reduce the freely  
168 dissolved concentration, i.e., by the partition constant between medium and air  
169  $K_{\text{medium/air}}$ . As Figure 1A indicates, only very hydrophilic chemicals showed a direct  
170 correlation between the  $K_{\text{medium/air}}$  and the air water partition constants  $K_{a/w}$  (dashed  
171 line). More hydrophobic chemicals such as 2-Phenylphenol, 4-Pentylphenol or 2,4,5-  
172 Trichloroaniline (Table 1, hydrophobicity expressed as  $\log K_{\text{lip/w}}$ ) deviated up to a factor  
173 of 10 from the one-to-one line indicated by a dotted horizontal line in Figure 1A and  
174 the deviation was slightly larger for the AhR-CALUX, AREc32 and ARE-BLA medium  
175 that contained a higher fraction of FBS, and therefore had a higher retaining capacity.

176 The vertical dotted line in Figure 1B indicates the  $K_{\text{medium/air}}$  cut-off of  $10^4$ , below  
177 which we had seen loss of chemicals and cross contamination of wells in our  
178 experiments as discussed above. This cut-off corresponds to 400 mL of air in  
179 equilibrium with the 40  $\mu\text{L}$  of medium to reach a one-to-one distribution between  
180 medium and air.



○ eneBLAzer

181  
182 Figure 1A. Medium-air partition constants  $K_{\text{medium/air}}$  plotted against air-water partition constants  $K_{a/w}$  for media with  
183 10% and 2% FBS (AhR-CALUX, AREc32 and ARE-BLA with medium consisting of 90% DMEM Glutamax with 10%



184 FBS (black diamonds) and the other GeneBLAzer assays with medium consisting of 98% Opti-MEM with 2% csFBS  
185 (open circles)). B. Volume of air to be equilibrated with 40  $\mu\text{L}$  of media (same symbols as in A) to reach a one-to-  
186 one distribution between the two phases (phase ratio  $V_{\text{medium}}:V_{\text{air}} = 1$  with  $V_{\text{medium}} = 40 \mu\text{L}$ ). The horizontal line in A  
187 and the vertical line in B mark the  $K_{\text{medium/air}}$  cut-off of  $10^4$ .

188 The cells have only a very minor contribution to the overall partitioning of  
189 chemicals within the well and will not change the picture substantially unless they are  
190 metabolized.<sup>9</sup> There is a difference between the different media used, the medium for  
191 AREc32 and AhR-CALUX is supplemented with 10% FBS, which has a higher sorptive  
192 capacity than the GeneBLAzer medium supplemented with 2% FBS and hence we can  
193 expect that more chemicals can be retained in the AREc32 and AhR-CALUX assays  
194 (Figure 1A).

195 It is interesting to compare Aniline, Quinoline and 2,4,5-Trichloroaniline: From  
196  $K_{\text{a/w}}$  alone one would expect that 2,4,5-Trichloroaniline would be lost and cross-  
197 contaminate neighboring wells, while the others pose less of a problem. This is not the  
198 case, it is just the other way around. As is shown below in section "Baseline toxicity  
199 QSARs", 2,4,5-Trichloroaniline was a valid contributor to the baseline toxicity QSARs  
200 of all eight cell lines. In contrast, Aniline and Quinoline contaminated neighboring wells  
201 so badly that all plates that contained those two chemicals could not be evaluated (data  
202 not shown). These two chemicals were excluded from further experiments altogether.  
203 The  $K_{\text{medium/air}}$  cut-off substantiates these empirical findings- 2,4,5-Trichloroaniline is  
204 above and Aniline and Quinoline are below the cut-off (Figure 1A).

205 The other semi-volatile chemicals with a log  $K_{\text{medium/air}}$  between 2 and 3 (Butan-  
206 1-ol, Pentan-1-ol, Nitrobenzene, Hexan-1-ol, 2-Nitrotoluene and N,N-Dimethylaniline)  
207 were mainly lost without a strong cross contamination and were therefore included in  
208 further experiments in order to use the baseline QSAR analysis to estimate the degree  
209 of loss. We did not attempt to measure the cytotoxicity of the remaining four chemicals  
210 with log  $K_{\text{medium/air}} < 2$ , they were only included in the thermodynamic analysis as  
211 reference. Note that Birch et al.<sup>25</sup> included a substantially higher number of such more  
212 volatile chemicals in their study of test substance losses and cross-over in 96-well  
213 plates.

214

215 **Loss processes to other system components.** The losses due to binding to the  
216 multi-well plates are expected to be negligible because we recently demonstrated that  
217 the binding to polystyrene will only become significant within the 24h exposure for  
218 medium that is not supplemented with FBS due to the substantially lower

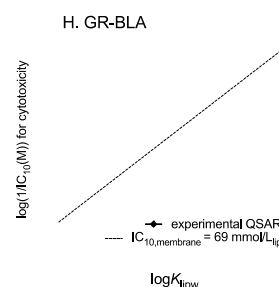
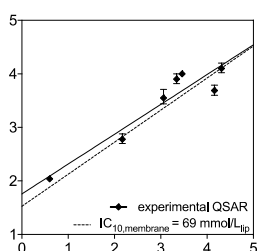
219  $K_{\text{polystyrene/medium}}$  than  $K_{\text{polystyrene/w}}$  and very slow diffusion coefficients of chemicals in  
220 polystyrene.<sup>11</sup>

221 Likewise the “loss” due to cellular uptake is negligible in absence of biotransformation  
222 in the overall mass balance with fractions of chemicals in cells (eq. 7) of 0.06 to 3.1%.  
223 As we will show below, this does not mean that the effective cellular concentrations  
224 are low but just that the volumes of proteins and lipids of the medium are much higher  
225 than that of the cells (Table 2). It is vital to differentiate between mass balances, i.e.,  
226 amounts and fractions in the different compartments, and concentrations in the  
227 different compartments (cell, medium, air).

228  
229 **Baseline toxicity QSARs.** All concentration-cytotoxicity curves are plotted in the SI,  
230 Section S7, Figures S7 to S14. We obtained valid  $IC_{10}$  (Table S3) for only 7 out of the  
231 19 chemicals in the dataset of Vaes et al.<sup>27</sup> after defining the  $K_{\text{medium/air}}$  cut-off. This  
232 data size is relatively small for regression analysis with two fit parameters per cell line.  
233 However the entire set of 51 valid  $IC_{10}$  can be used to evaluate if critical membrane  
234 concentrations are constant across chemicals and cell lines.

235 All baseline QSARs are depicted in Figure 2 and the QSAR equations are given in  
236 Table 3. As anticipated, the QSARs of all tested cell lines were similar. The additional  
237 chemicals tested around the volatility cut-off are discussed in Section S8, some are  
238 still within the QSAR but they are clearly starting to get lost and were therefore not  
239 included in the QSAR training set.

240



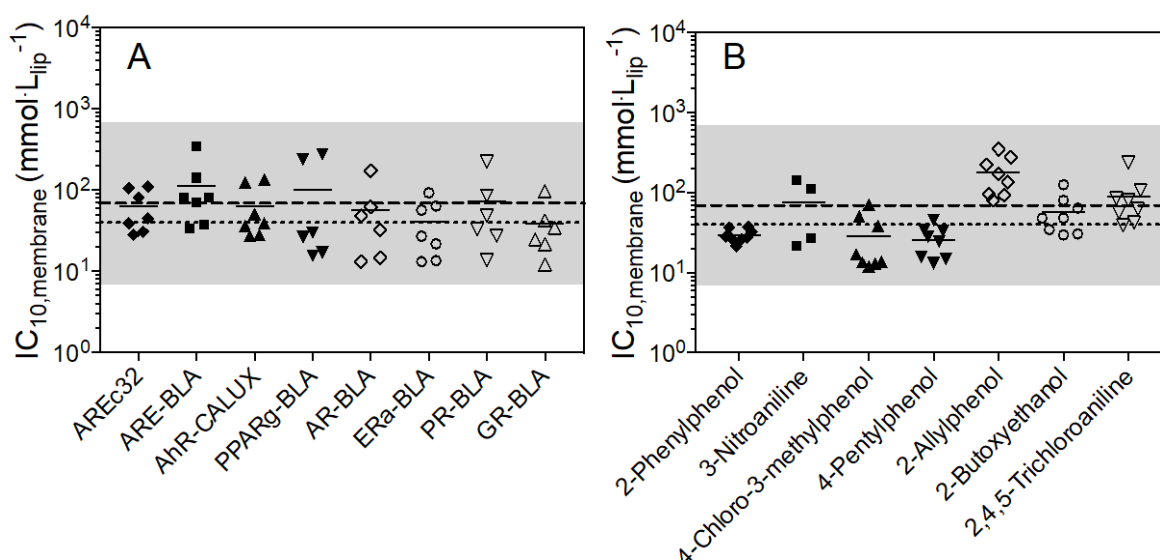
241

242 Figure 2. QSARs for baseline toxicity for all cell lines. The solid lines correspond to the best fit (equations are given  
 243 in Table 3) and the dotted lines are the predicted  $IC_{10}$  and associated QSAR for the mass balance model, calculated  
 244 with an internal critical membrane concentration of 69  $mmol/L_{lip}$ .

245  
 246 Table 3. QSARs for baseline toxicity for all cell lines of the form  $\log(1/IC_{10}(M)) = slope \cdot \log K_{lipw} + intercept$ . If  $n = 6$ ,  
 247 3-Nitroaniline had to be excluded due to poor quality of the concentration-inhibition curves..

Reporter gene cell line	Slope	intercept	R <sup>2</sup>	n
AREc32	0.56±0.09	1.76±0.28	0.8906	7
ARE-BLA	0.68±0.08	1.19±0.26	0.9350	7
AhR-CALUX	0.73±0.10	1.28±0.31	0.9181	7
PPAR $\gamma$ -BLA	0.64±0.20	1.71±0.69	0.9523	6
AR-BLA	0.76±0.14	1.44±0.49	0.8755	6
ER $\alpha$ -BLA	0.76±0.10	1.54±0.42	0.8762	7
PR-BLA	0.70±0.16	1.52±0.11	0.8283	6
GR-BLA	0.72±0.13	1.67±0.42	0.8943	6

248  
 249 **Critical membrane concentrations.** The critical membrane concentrations  
 250  $IC_{10,membrane}$  were calculated from nominal  $IC_{10}$  by eqn. 7, 8 9 and 10. As Figure 3A  
 251 shows, there was no significant difference in  $IC_{10,membrane}$  between cell lines (ANOVA,  
 252  $F=0.7853$ ,  $P=0.6168$ ) with a mean  $IC_{10,membrane}$  of 69  $mmol \cdot L_{lip}^{-1}$  (95% CI; 49 to 89) and  
 253 a median of 40  $mmol \cdot L_{lip}^{-1}$ .



254  
 255 Figure 3. The critical membrane concentration  $IC_{10,membrane}$  calculated from the measured  $IC_{10}$  using the mass  
 256 balance model in the wells (eqs. 7-8) and the mass balance in the cells (eqs. 9-10). The short lines are the means

257 of the individual cell lines, the broken line is the mean of all data and the dotted line corresponds to the median.  
258 The grey bands correspond to a factor of 10 in each direction. A.  $IC_{10,membrane}$  binned according to cell line, B.  
259  $IC_{10,membrane}$  binned according to chemical.

260  
261 For comparison the critical membrane burdens for 50% mortality  $ILC_{50}$  were 118  
262  $mmol \cdot kg_{lip}^{-1}$  (95% CI 64 to 173) for daphnia and 108  $mmol \cdot kg_{lip}^{-1}$  (95% CI 73 to 143) for  
263 fish.<sup>31</sup> Note the different units but in the literature the density of lipids is often assumed  
264 to be 1  $kg_{lip} \cdot Lip^{-1}$  and hence the units can be used interchangeably. Although  
265 concentration response curves are not expected to be linear up to 50% effect but rather  
266 turn into a log-sigmoidal form above 30-40% of effect,<sup>48</sup> we can roughly estimate the  
267  $IC_{50,membrane}$  in the investigated cells as 345  $mmol \cdot kg_{lip}^{-1}$ . The 95% CI of the  $ILC_{50}$  for  
268 aquatic animals are overlapping with the 95% CI of the cytotoxicity  $IC_{10,membrane}$  and  
269 are only slightly lower than the estimated  $IC_{50,membrane}$ . It is interesting to note but does  
270 not come as a surprise that cytotoxicity in cell lines and lethality to aquatic organisms  
271 occurred at similar exposure levels. In the luminescent bacteria *Aliivibrio fischeri* 50%  
272 cytotoxicity occurred at a modelled membrane burden of approximately 200  $mmol \cdot kg_{lip}^{-1}$ .  
273 This difference of a factor of two can be rationalized by the difference in effect level  
274 and by the much shorter exposure with *A. fischeri*, which was 30 min, while cytotoxicity  
275 toward human and rat cells was assessed after 24h in the present study.

276 A subset of Vaes' baseline toxicants<sup>27</sup> and additional chemicals were also tested for  
277 their effect to accelerate the decay of the membrane potential in isolated energy-  
278 transducing membranes, which is an indicator of the disturbance of membrane  
279 structure.<sup>53</sup> In that study, an effective membrane concentration of 300  $mmol \cdot kg_{lip}^{-1}$  lead  
280 to the critical effect, independent if polar or nonpolar or even charged organic  
281 compounds were tested, confirming the hypothesis of common mechanism of action  
282 of nonpolar and polar chemicals.

283 Due to the volatility cut-off, we could include only one of the nonpolar baseline toxicants  
284 of the initial set of Vaes' baseline toxicants.<sup>27</sup> This was Butoxyethanol, which was  
285 statistically not different from the other chemicals (t-test,  $P=0.4278$ , Welch-corrected  
286  $t=0.8066$ ,  $df=23.93$ ). Butoxyethanol had a narrower confidence band and lay overall  
287 closer to the mean and median than the other tested chemicals (Figure 3B).

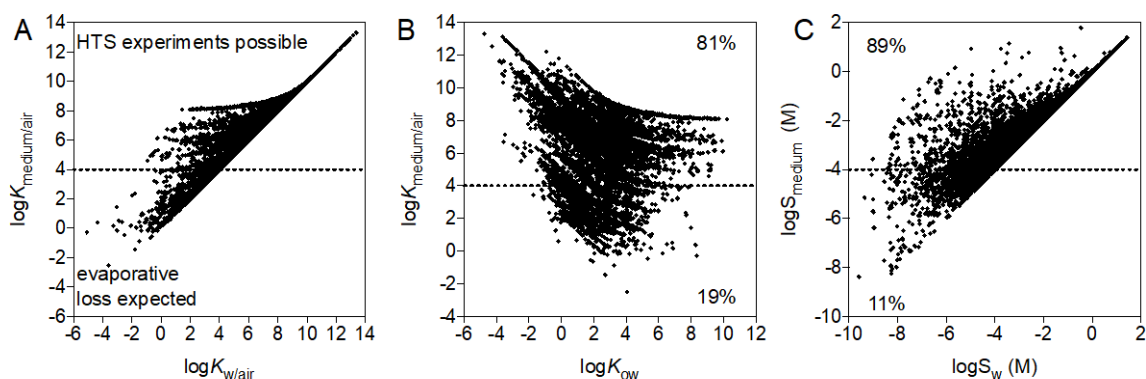
288 We can use the QSARs to predict nominal  $IC_{10}$  but an alternative approach is to  
289 backtrack eqs. 8-13 to derive expected cytotoxicity concentrations  $IC_{10}$  from the  
290 constant critical membrane burdens of approximately 70  $mmol \cdot kg_{lip}^{-1}$ . Calculating the

291 IC<sub>10</sub> either way prior to an experiment can also help define appropriate dosing  
292 concentrations, interpret toxicity data and support drug discovery.

293

294 **Implications of the volatility cut-off for HTS.** On first sight, the volatility cut-off  
295 appears at a quite high  $K_{\text{medium}/w}$ . For each 10000 molecules in medium one is in air (at  
296 equal compartment sizes) and still those chemicals escape the system. We analyzed  
297 the list of 8947 chemicals tested in Tox21<sup>49</sup> to identify how many of the chemicals that  
298 were included in Tox21 are likely to be lost while performing an bioassay experiment.  
299 This is only a thought experiment, the conditions under which the Tox21 assays were  
300 run, might have differed substantially from the setup that was applied to define the  
301 volatility cut-off but is useful to estimate the dimension of the problem associated to  
302 potential loss of chemicals in HTS systems.

303 As Figure 4A demonstrates, medium containing 10% FBS can retain some  
304 chemicals and the  $K_{\text{medium}/\text{air}}$  can be orders of magnitude higher than the  $K_{w/\text{air}}$ . 81% of  
305 the Tox21 chemicals were above the threshold of  $\log K_{\text{medium}/\text{air}} = 4$  (Figure 4B), and  
306 hence can be tested without any expected significant loss but the 19% that are below  
307 this threshold might have been partially lost. The  $K_{\text{medium}/\text{air}}$  is not directly related to the  
308  $K_{ow}$  (Figure 4B), and this is why the effect of the medium on  $K_{\text{medium}/\text{air}}$  can be stronger  
309 or weaker depending on the  $K_{ow}$ .



310

311 *Figure 4. A. Relationship between  $K_{\text{medium}/\text{air}}$  and  $K_{w/\text{air}}$  to demonstrate the retaining effect of medium. B. No*  
312 *relationship between the  $K_{\text{medium}/\text{air}}$  cut-off and hydrophobicity, expressed as  $\log K_{ow}$ . C. 89% of all chemicals had a*  
313 *solubility in medium above 100  $\mu\text{M}$  and the solubility enhancement by medium components is dependent on the*  
314 *medium compositions (calculations in the figure for 10 % FBS).*

315

316 **Implications of the baseline toxicity QSAR for dosing in HTS.** In Tox21, chemicals  
317 were dosed from DMSO stocks to a maximum concentration of 100  $\mu\text{M}$  in the final  
318 volume of 6  $\mu\text{L}$  in the bioassays. We calculated, at which  $\log K_{\text{lip}/w}$  the IC<sub>10</sub>(QSAR)

319 would be 100  $\mu\text{M}$  using the QSAR equations in Table 3, which comes to  $\log K_{\text{ip/w}}$  3.1 to  
320 4.1 depending on the cell line. That means that chemicals with a  $\log K_{\text{ip/w}}$  below 3.1 to  
321 4.1 were not tested up to their minimum toxicity if they were tested up to 100  $\mu\text{M}$ .  
322 Cytotoxicity or effects occurring at rather high concentrations but still below baseline  
323 toxicity would not be detected (false negative).

324 On the other end of the spectrum, hydrophobic chemicals with  $\log K_{\text{ip/w}} > 4$  could  
325 easily be accidentally overdosed if dosed up to 100  $\mu\text{M}$  and might have precipitated in  
326 the bioassay. Not all chemicals are expected to be soluble at their baseline-toxic  
327 concentration. Especially hydrophobic chemicals with high melting point can often not  
328 be dosed up to concentrations where baseline toxicity would occur.<sup>54</sup> It is possible to  
329 estimate the solubility in bioassay medium from the aqueous solubility  $S_w$  by  
330 multiplying with the  $K_{\text{medium/w}}$ .<sup>52</sup> As Figure 4C shows, the medium solubility  $S_{\text{medium}}$  can  
331 be much higher than the  $S_w$  (calculations performed for medium with 10% FBS). Dosing  
332 at  $S_w$  risks again a false negative result because the medium enhances apparent  
333 solubility but also binds most of the dosed chemicals, hence one should rather aim at  
334 dosing up to  $S_{\text{medium}}$ . 89% of all Tox21 chemicals had a  $S_{\text{medium}} > 100 \mu\text{M}$  and could  
335 have dosed higher in some of the assays.

336 One must keep in mind that the models presented here will have highest  
337 predictability for exactly the same experimental setups but can provide a guidance for  
338 similar bioassays and HTS set ups.

339

## 340 CONCLUSION

341 The analysis presented here will help to further improve HTS using reporter gene  
342 assays. HTS bioassays that use automated liquid handling or the D300 dispenser  
343 require multi-well plates to be open during handling. Also during incubation, the plates  
344 are typically not fully sealed but just covered with a plastic lid or a breathable sealant  
345 plus a plastic lid. We have demonstrated earlier that the same assays can also be run  
346 in a headspace-free set up<sup>22</sup> or with a defined headspace.<sup>21</sup> However, manual injection  
347 with syringes of the volatile chemicals is labor-intensive, oxygen deficiency can impact  
348 cell viability and it can also be challenging to keep  $\text{CO}_2$  concentrations and pH constant  
349 in closed tests.<sup>22</sup> Systems with defined headspace have been successfully applied to  
350 biodegradation testing<sup>55, 56</sup> and have potential to be adapted to *in vitro* bioassays.

351 Paying attention to the volatility cut-off in routine HTS set ups can help to avoid artifacts  
352 and false negative results.

353 We refined a previously proposed Henry coefficient cut-off by accounting for the  
354 binding of chemicals to medium components, which retains chemicals in the assay  
355 system and defined a new robust  $K_{\text{medium/air}}$  cut-off of 10000 L/L. Evidently, loss to the  
356 air is not the only loss process possible in HTS cell assays. Additional consideration  
357 should be given to the stability of chemicals in the test medium and binding to plastic  
358 multi-well plates.

359 Instead of dosing all chemicals at the same maximum concentration, it is more  
360 preferable to adjust dosing to the physicochemical properties and expected baseline  
361 toxic effects of the specific chemical and to dose up to or slightly exceeding what is  
362 predicted from the baseline toxicity QSARs. This might be logistically challenging and  
363 not possible for practical reasons in large HTS setups but it would be at least useful to  
364 bin chemicals into groups with physicochemical properties and test the bins in different  
365 ranges. By comparing experimental cytotoxicity with the QSAR, we can find out if the  
366 cytotoxicity is caused by baseline toxicity or occurs at much lower concentrations,  
367 which would then point to a specific mode of action.

368

## 369 ASSOCIATED CONTENT

### 370 **Supporting Information**

371 The Supporting Information is available free of charge on the ACS Publications website  
372 at doi:xxxxxx. Additional sections on chemicals, the dosing procedures and the  
373 bioassay workflow, comparison of cell viability testing using the Presto Blue<sup>®</sup> assay  
374 and live-cell imaging, comparison of dosing with the digital dispenser with automated  
375 pipetting, loss processes to the air and contamination of neighboring wells, all  
376 concentration-response curves of all test chemicals in all assays and supplementary  
377 analyses.

378

## 379 AUTHOR INFORMATION

### 380 **Corresponding Author**

381 \*Phone: +49 341 235-1244. Fax: +49 341 235-1787. E-mail: beate.escher@ufz.de

### 382 **ORCID**

383 Beate Escher: 0000-0002-5304-706X

384 **Funding**

385 We gratefully acknowledge the financial support by the CEFIC Long-Range Research  
386 Initiative (LRI), project ECO36. The robotic HTS systems and the D300 dispenser are  
387 a part of the major infrastructure initiative CITEPro (Chemicals in the Terrestrial  
388 Environment Profiler) funded by the Helmholtz Association with co-funding by the  
389 States of Saxony and Saxony-Anhalt.

390 **Notes**

391 The authors declare no competing financial interest.

392

393 **ACKNOWLEDGMENTS**

394 We thank Christin Kühnert (UFZ) for experimental support. We thank Cedric Abele  
395 (UFZ), Mark Cronin (LJMU, UK), Satoshi Endo (NIES, Japan), Fabian Fischer (UFZ),  
396 Todd Gouin (TG Environmental Research, UK), Joop Hermens, IRAS, Utrecht  
397 University, the Netherlands) and Luise Henneberger (UFZ) for helpful discussions  
398 including review of the manuscript.

399

400 **REFERENCES**

- 401 1. Collins, F.; Gray, G. N.; Bucher, J. R., Transforming environmental health  
402 protection. *Science* **2008**, *319*, 906-907.
- 403 2. Betts, K. S., Tox21 to Date Steps toward Modernizing Human Hazard  
404 Characterization. *Environ. Health Perspect.* **2013**, *121*, (7), A228-A228.
- 405 3. Wetmore, B. A., Quantitative in vitro-to-in vivo extrapolation in a high-throughput  
406 environment. *Toxicology* **2015**, *332*, 94-101.
- 407 4. Heringa, M. B.; Schreurs, R.; van der Saag, P. T.; van der Burg, B.; Hermens,  
408 J. L. M., Measurement of free concentration as a more intrinsic dose parameter in an  
409 in vitro assay for estrogenic activity. *Chem. Res. Toxicol.* **2003**, *16*, (12), 1662-1663.
- 410 5. Henneberger, L.; Mühlenbrink, M.; König, M.; Schlichting, R.; Fischer, F. C.;  
411 Escher, B. I., Quantification of freely dissolved effect concentrations in in vitro cell-  
412 based bioassays. *Arch. Toxicol.* **2019**, accepted 17 June 2019,  
413 <https://doi.org/10.1007/s00204-019-02498-3>.
- 414 6. Tice, R. R.; Austin, C. P.; Kavlock, R. J.; Bucher, J. R., Improving the Human  
415 Hazard Characterization of Chemicals: A Tox21 Update. *Environ. Health Perspect.*  
416 **2013**, *121*, (7), 756-765.



- 417 7. Jahnke, A.; Mayer, P.; Schaefer, S.; Witt, G.; Haase, N.; Escher, B. I., Strategies  
418 for Transferring Mixtures of Organic Contaminants from Aquatic Environments into  
419 Bioassays. *Environ. Sci. Technol.* **2016**, *50*, (11), 5424-5431.
- 420 8. Armitage, J. M.; Wania, F.; Arnot, J. A., Application of mass balance models  
421 and the chemical activity concept to facilitate the use of in vitro toxicity data for risk  
422 assessment. *Environ. Sci. Technol.* **2014**, *48*, 9770–9779.
- 423 9. Fischer, F.; Henneberger, L.; König, M.; Bittermann, K.; Linden, L.; Goss, K.-U.;  
424 Escher, B., Modeling exposure in the Tox21 in vitro bioassays. *Chem. Res. Toxicol.*  
425 **2017**, *30*, 1197–1208.
- 426 10. Fischer, F.; Abele, C.; Droge, S. T. J.; Henneberger, L.; König, M.; Schlichting,  
427 R.; Scholz, S.; Escher, B., Cellular Uptake Kinetics of Neutral and Charged Chemicals  
428 in inVitro Assays Measured by Fluorescence Microscopy. *Chem. Res. Toxicol.* **2018**,  
429 *31*, 646-657.
- 430 11. Fischer, F. C.; Cirpka, O.; Goss, K. U.; Henneberger, L.; Escher, B. I.,  
431 Application of experimental polystyrene partition constants and diffusion coefficients to  
432 predict the sorption of organic chemicals to well plates in in vitro bioassays. *Environ.*  
433 *Sci. Technol.* **2018**, *52*, 13511-13522.
- 434 12. Judson, R.; Houck, K.; Martin, M.; Richard, A. M.; Knudsen, T. B.; Shah, I.; Little,  
435 S.; Wambaugh, J.; Setzer, R. W.; Kothya, P.; Phuong, J.; Filer, D.; Smith, D.; Reif, D.;  
436 Rotroff, D.; Kleinstreuer, N.; Sipes, N.; Xia, M. H.; Huang, R. L.; Crofton, K.; Thomas,  
437 R. S., Analysis of the Effects of Cell Stress and Cytotoxicity on In Vitro Assay Activity  
438 Across a Diverse Chemical and Assay Space. *Tox. Sci.* **2016**, *152*, (2), 323-339.
- 439 13. Fay, K. A.; Villeneuve, D. L.; Swintek, J.; Edwards, S. W.; Nelms, M. D.;  
440 Blackwell, B. R.; Ankley, G. T., Differentiating Pathway-Specific From Nonspecific  
441 Effects in High-Throughput Toxicity Data: A Foundation for Prioritizing Adverse  
442 Outcome Pathway Development. *Tox. Sci.* **2018**, *163*, (2), 500-515.
- 443 14. Adan, A.; Kiraz, Y.; Baran, Y., Cell Proliferation and Cytotoxicity Assays. *Current*  
444 *Pharmaceutical Biotechnology* **2016**, *17*, (14), 1213-1221.
- 445 15. Ramirez, C. N.; Antczak, C.; Djaballah, H., Cell viability assessment: toward  
446 content-rich platforms. *Expert Opinion on Drug Discovery* **2010**, *5*, (3), 223-233.
- 447 16. Nivala, J.; Neale, P. A.; Haasis, T.; Kahl, S.; König, M.; Müller, R.; Reemtsma,  
448 T.; Schlichting, R.; Escher, B., Application of bioanalytical tools to evaluate treatment  
449 efficacy of conventional and intensified treatment wetlands. *Environ. Sci.: Water Res.*  
450 *Technol.* **2018**, *4*, 206-217.

- 451 17. McDermott, C.; Allshire, A.; van Pelt, F.; Heffron, J. J. A., Validation of a method  
452 for acute and subchronic exposure of cells in vitro to volatile organic solvents. *Toxicol.*  
453 *in Vitro* **2007**, *21*, (1), 116-124.
- 454 18. Aufderheide, M.; Halter, B.; Mohle, N.; Hochrainer, D., The CULTEX RFS: A  
455 Comprehensive Technical Approach for the In Vitro Exposure of Airway Epithelial Cells  
456 to the Particulate Matter at the Air-Liquid Interface. *Biomed Research International*  
457 **2013**.
- 458 19. Liu, F. F.; Escher, B. I.; Were, S.; Duffy, L.; Ng, J. C., Mixture Effects of  
459 Benzene, Toluene, Ethylbenzene, and Xylenes (BTEX) on Lung Carcinoma Cells via  
460 a Hanging Drop Air Exposure System. *Chem. Res. Toxicol.* **2014**, *27*, (6), 952-959.
- 461 20. Liu, F. F.; Peng, C.; Escher, B. I.; Fantino, E.; Giles, C.; Were, S.; Duffy, L.; Ng,  
462 J. C., Hanging drop: an in vitro air toxic exposure model using human lung cells in 2D  
463 and 3D structures *J. Hazard. Mater.* **2013**, *261*, 701-710.
- 464 21. Harder, A.; Escher, B. I.; Landini, P.; Tobler, N. B.; Schwarzenbach, R. P.,  
465 Evaluation of bioanalytical tools for toxicity assessment and mode of toxic action  
466 classification of reactive chemicals. *Environ. Sci. Technol.* **2003**, *37*, (21), 4962-4970.
- 467 22. Stalter, D.; Dutt, M.; Escher, B. I., Headspace-free setup of in vitro bioassays  
468 for the evaluation of volatile disinfection by-products. *Chem. Res. Toxicol.* **2013**, *26*,  
469 1605–1614.
- 470 23. Stalter, D.; O'Malley, E.; von Gunten, U.; Escher, B. I., Fingerprinting the  
471 reactive toxicity pathways of 50 drinking water disinfection by-products. *Water Res.*  
472 **2016**, *91*, 19-30.
- 473 24. Henneberger, L.; Mühlenbrink, M.; Fischer, F. C.; Escher, B. I., C18-Coated  
474 Solid-Phase Microextraction Fibers for the Quantification of Partitioning of Organic  
475 Acids to Proteins, Lipids, and Cells. *Chem. Res. Toxicol.* **2019**, *32*, (1), 168 - 178.
- 476 25. Birch, H.; Kramer, N. I.; Mayer, P., Time-Resolved Freely Dissolved  
477 Concentrations of Semi-Volatile and Hydrophobic Test Chemicals in *In Vitro* Assays –  
478 Measuring High Losses and Cross-Over by Headspace Solid-Phase Microextraction.  
479 *Chem. Res. Toxicol.* **2019**, submitted to CRT.
- 480 26. Jones, R. E.; Zheng, W.; McKew, J. C.; Chen, C. Z., An Alternative Direct  
481 Compound Dispensing Method Using the HP D300 Digital Dispenser. *Jala* **2013**, *18*,  
482 (5), 367-374.

- 483 27. Vaes, W. H. J.; Ramos, E. U.; Verhaar, H. J. M.; Hermens, J. L. M., Acute  
484 toxicity of nonpolar versus polar narcosis: Is there a difference? *Environ. Toxicol.*  
485 *Chem.* **1998**, *17*, (7), 1380-1384.
- 486 28. Vaes, W. H. J.; Ramos, E. U.; Hamwijk, C.; vanHolsteijn, I.; Blaauboer, B. J.;  
487 Seinen, W.; Verhaar, H. J. M.; Hermens, J. L. M., Solid phase microextraction as a tool  
488 to determine membrane/water partition coefficients and bioavailable concentrations in  
489 in vitro systems. *Chem. Res. Toxicol.* **1997**, *10*, (10), 1067-1072.
- 490 29. Urrestarazu Ramos, E.; Vaes, W. H. J.; Verhaar, H. J. M.; Hermens, J. L. M.,  
491 Quantitative structure-activity relationships for the aquatic toxicity of polar and  
492 nonpolar narcotic pollutants. *J. Chem. Inf. Comput. Sci.* **1998**, *38*, (5), 845-852.
- 493 30. Klüver, N.; Vogs, C.; Altenburger, R.; Escher, B. I.; Scholz, S., Development of  
494 a general baseline toxicity QSAR model for the fish embryo acute toxicity test.  
495 *Chemosphere* **2016**, *164*, 164-173.
- 496 31. Escher, B. I.; Schwarzenbach, R. P., Mechanistic studies on baseline toxicity  
497 and uncoupling of organic compounds as a basis for modeling effective membrane  
498 concentrations in aquatic organisms. *Aquatic Sciences* **2002**, *64*, (1), 20-35.
- 499 32. Escher, B. I.; Bramaz, N.; Mueller, J. F.; Quayle, P.; Rutishauser, S.;  
500 Vermeirssen, E. L. M., Toxic equivalent concentrations (TEQs) for baseline toxicity and  
501 specific modes of action as a tool to improve interpretation of ecotoxicity testing of  
502 environmental samples. *J. Env. Monitor.* **2008**, *10*, (5), 612-621.
- 503 33. Escher, B.; Baumer, A.; Bittermann, K.; Henneberger, L.; König, M.; Kühnert,  
504 C.; Klüver, N., General baseline toxicity QSAR for non-polar, polar and ionisable  
505 chemicals and their mixtures in the bioluminescence inhibition assay with *Allivibrio*  
506 *fischeri*. *Environmental Science: Processes & Impacts* **2017**, *19*, 414-428.
- 507 34. Schwarzenbach, R. P.; Gschwend, P. M.; Imboden, D. M., *Environmental*  
508 *Organic Chemistry, third edition*. Wiley: New York, NY, USA, 2016.
- 509 35. Endo, S.; Goss, K. U., Serum Albumin Binding of Structurally Diverse Neutral  
510 Organic Compounds: Data and Models. *Chem. Res. Toxicol.* **2011**, *45*, (24), 2293-  
511 2301.
- 512 36. Ulrich, N.; Endo, S.; Brown, T. N.; Watanabe, N.; Bronner, G.; Abraham, M. H.;  
513 Goss, K.-U., UFZ-LSER database v 3.2.1 [Internet], Leipzig, Germany, Helmholtz  
514 Centre for Environmental Research-UFZ. 2017 [accessed on 26.09.2018]. Available  
515 from <http://www.ufz.de/lserd> **2018**.

- 516 37. Goss, K. U., Prediction of the temperature dependency of Henry's law constant  
517 using poly-parameter linear free energy relationships. *Chemosphere* **2006**, *64*, (8),  
518 1369-1374.
- 519 38. Shukla, S. J.; Huang, R. L.; Sommons, S. O.; Tice, R. R.; Witt, K. L.; vanLeer,  
520 D.; Rabamabhardan, R.; Austin, C. P.; Xia, M. H., Profiling environmental chemicals  
521 for activity in the antioxidant response element signaling pathway using a high-  
522 throughput screening approach. *Environ Health Perspect* **2012**, *120*, (8), 1150–1156.
- 523 39. Huang, R. L.; Xia, M. H.; Cho, M. H.; Sakamuru, S.; Shinn, P.; Houck, K. A.;  
524 Dix, D. J.; Judson, R. S.; Witt, K. L.; Kavlock, R. J.; Tice, R. R.; Austin, C. P., Chemical  
525 genomics profiling of environmental chemical modulation of human nuclear receptors.  
526 *Environ. Health Perspect.* **2011**, *119*, (8), 1142-1148.
- 527 40. Wang, X. J., Hayes, J.D., and Wolf, C.R., Generation of a stable antioxidant  
528 response element–driven reporter gene cell line and its use to show redox-dependent  
529 activation of Nrf2 by cancer chemotherapeutic agents. *Cancer Res.* **2006**, *66*, (22),  
530 10983-10994.
- 531 41. Brennan, J. C.; He, G.; Tsutsumi, T.; Zhao, J.; Wirth, E.; Fulton, M. H.; Denison,  
532 M. S., Development of Species-Specific Ah Receptor-Responsive Third Generation  
533 CALUX Cell Lines with Enhanced Responsiveness and Improved Detection Limits.  
534 *Environ. Sci. Technol.* **2015**, *49*, (19), 11903-11912.
- 535 42. Escher, B. I.; Dutt, M.; Maylin, E.; Tang, J. Y. M.; Toze, S.; Wolf, C. R.; Lang,  
536 M., Water quality assessment using the AREc32 reporter gene assay indicative of the  
537 oxidative stress response pathway. *J. Environ. Monitor.* **2012**, *14*, (11), 2877-85.
- 538 43. König, M.; Escher, B. I.; Neale, P. A.; Krauss, M.; Hilscherová, K.; Novák, J.;  
539 Teodorović, I.; Schulze, T.; Seidensticker, S.; Kamal Hashmi, M. A.; Ahlheim, J.; Brack,  
540 W., Impact of untreated wastewater on a major European river evaluated with a  
541 combination of *in vitro* bioassays and chemical analysis. *Environ. Pollut.* **2017**, *220*,  
542 1220-1230.
- 543 44. Neale, P. A.; Altenburger, R.; Ait-Aissa, S.; Brion, F.; Busch, W.; de Aragão  
544 Umbuzeiro, G.; Denison, M. S.; Du Pasquier, D.; Hilscherova, K.; Hollert, H.; Morales,  
545 D. A.; Novac, J.; Schlichting, R.; Seiler, T.-B.; Serra, H.; Shao, Y.; Tindall, A. J.;  
546 Tollefsen, K. E.; Williams, T. D.; Escher, B. I., Development of a bioanalytical test  
547 battery for water quality monitoring: Fingerprinting identified micropollutants and their  
548 contribution to effects in surface water. *Water Res.* **2017**, *123*, 734-750.

- 549 45. Cassaday, J.; Finley, M.; Squadroni, B.; Jezequel-Sur, S.; Rauch, A.; Gajera,  
550 B.; Uebele, V.; Hermes, J.; Zuck, P., Development of a Platform to Enable Fully  
551 Automated Cross-Titration Experiments. *SLAS Technol.* **2016**, *22*, (2), 195-205.
- 552 46. Smith, K. P.; Brennan-Krohn, T.; Weir, S.; Kirby, J. E., Improved Accuracy of  
553 Cefepime Susceptibility Testing for Extended-Spectrum-Beta-Lactamase-Producing  
554 Enterobacteriaceae with an On-Demand Digital Dispensing Method. *Journal of Clinical*  
555 *Microbiology* **2017**, *55*, (2), 470-478.
- 556 47. Neale, P. A.; Brack, W.; Ait-Aissa, S.; Busch, W.; Hollender, J.; Krauss, M.;  
557 Maillot-Maréchal, E.; Munz, N. A.; Schlichting, R.; Schulze, T.; Vogler, B.; Escher, B.,  
558 Solid-phase extraction as sample preparation of water samples for cell-based and  
559 other *in vitro* bioassays. *Environ. Sci. Process. Impacts* **2018**, *20*, 493-504.
- 560 48. Escher, B.; Neale, P. A.; Villeneuve, D., The advantages of linear concentration-  
561 response curves for *in vitro* bioassays with environmental samples. *Environ. Toxicol.*  
562 *Chem.* **2018**, *37*, (9), 2273–2280.
- 563 49. US EPA, TOX21SL: Tox21 Screening Library. **2019**,  
564 [https://comptox.epa.gov/dashboard/chemical\\_lists/TOX21SL](https://comptox.epa.gov/dashboard/chemical_lists/TOX21SL), accessed on 22 March  
565 2019.
- 566 50. US EPA, Chemistry Dashboard. **2019**, <https://comptox.epa.gov/dashboard/>  
567 accessed on 22 March 2019.
- 568 51. Mansouri, K.; Grulke, C.; Judson, R.; Williams, A., OPERA: A QSAR tool for  
569 physicochemical properties and environmental fate predictions. *Abstr. Pap. Am.*  
570 *Chem. Soc.* **2017**, 253.
- 571 52. Fischer, F.; Henneberger, L.; Schlichting, R.; Escher, B., How to improve the  
572 dosing of chemicals in high-throughput *in vitro* mammalian cell assays. *Chem. Res.*  
573 *Toxicol.* **2019**, submitted.
- 574 53. Escher, B. I.; Eggen, R. I. L.; Schreiber, U.; Schreiber, Z.; Vye, E.; Wisner, B.;  
575 Schwarzenbach, R. P., Baseline toxicity (narcosis) of organic chemicals determined  
576 by *in vitro* membrane potential measurements in energy-transducing membranes.  
577 *Environ. Sci. Technol.* **2002**, *36*, (9), 1971-1979.
- 578 54. Mayer, P.; Reichenberg, F., Can highly hydrophobic organic substances cause  
579 aquatic baseline toxicity and can they contribute to mixture toxicity? *Environ. Toxicol.*  
580 *Chem.* **2006**, *25*, (10), 2639-2644.

- 581 55. Birch, H.; Anderson, H. R.; Comber, M.; Mayer, P., Biodegradation testing of  
582 chemicals with high Henry's constants separating mass and effective concentration  
583 reveals higher rate constants. *Chemosphere* **2017**, *174*, 716-721.
- 584 56. Birch, H.; Hammershøj, R.; Mayer, P., Determining Biodegradation Kinetics of  
585 Hydrocarbons at Low Concentrations: Covering 5 and 9 Orders of Magnitude of  $K_{ow}$   
586 and  $K_{aw}$ . *Environ. Sci. Technol.* **2018**, *52*, (4), 2143–2151.
- 587